DOI: 10.1002/chem.200601742

Evidence for a S_N2-Type Pathway for Phosphine Exchange in Phosphine–Phosphenium Cations, $[R_2P{-}PR'_3]^+$

John M. Slattery,[a] Cheryl Fish,[a] Michael Green,*[a] Thomas N. Hooper,[a] John C. Jeffery,[a] Richard J. Kilby,[a] Jason M. Lynam,[b] John E. McGrady,*[c] Dimitrios A. Pantazis,[c] Christopher A. Russell,*[a] and Charlotte E. Willans[b]

Abstract: Abstraction of a Cl^- ion from the *P*-chlorophospholes, R_4C_4PCl (R = Me, Et), produced the P–P bonded cations $[R_4C_4P{-}P(Cl)C_4R_4]^+$, which reacted with PPh_3 to afford X-ray crystallographically characterised phosphine–phosphenium cations $[R_4C_4P(PPh_3)]^+$ (R = Me, Et). Examination of the $^{31}P\{^1H\}$ NMR spectrum of a solution (CH_2Cl_2) of $[Et_4C_4P(PPh_3)]^+$ and PPh_3 revealed broadening of the resonances due to both free and coordinated PPh_3, and importantly it proved possible to measure the rate of exchange between PPh_3 and $[Et_4C_4P(PPh_3)]^+$ by line shape analysis (gNMR programmes). The results established second-order kinetics with $\Delta S^{\neq} = (-106.3 \pm 6.7)\ J\,mol^{-1}\,K^{-1}$, $\Delta H^{\neq} = (14.9 \pm 1.6)\ kJ\,mol^{-1}$ and $\Delta G^{\neq}(298.15\ K) = (46.6 \pm 2.6)\ kJ\,mol^{-1}$, values consistent with a S_N2-type pathway for the exchange process. This result contrasts with the dominant dissociative (S_N1-type) pathway reported for the analogous exchange reactions of the $[ArNCH_2CH_2N(Ar)P(PMe_3)]^+$ ion, and to understand in more detail the factors controlling these two different reaction pathways, we have analysed the potential energy surfaces using density functional theory (DFT). The calculations reveal that, whilst phosphine exchange in $[Et_4C_4P(PPh_3)]^+$ and $[ArNCH_2CH_2N(Ar)P(PMe_3)]^+$ is superficially similar, the two cations differ significantly in both their electronic and steric requirements. The high electrophilicity of the phosphorus center in $[Et_4C_4P]^+$, combined with strong π–π interactions between the ring and the incoming and outgoing phenyl groups of PPh_3, favours the S_N2-type over the S_N1-type pathway in $[Et_4C_4P(PPh_3)]^+$. Effective π-donation from the amide groups reduces the intrinsic electrophilicity of $[ArNCH_2CH_2N(Ar)P]^+$, which, when combined with the steric bulk of the aryl groups, shifts the mechanism in favour of a dissociative S_N1-type pathway.

Keywords: carbene homologues · cations · density functional calculations · phosphorus · structure elucidation

Introduction

The coordination chemistry of phosphorus is traditionally taught solely in terms of the donor–acceptor behaviour of trivalent, tricoordinate (σ^3,λ^3) phosphines. However, in recent years there have been substantial advances in the chemistry of low-coordinate (σ^2,λ^2) cationic phosphorus ligands of type $[R_2P]^+$, which can behave as electron-rich (i.e., lone-pair bearing) Lewis acids.[1] An interesting analogy that adds topicality to this subject is that these ligands are formally isolobal to carbenes whose chemistry has attracted considerable attention in recent years.[2,3] Experimentally, the chemistry of two classes of phosphenium ligands has been explored extensively: i) those where the phosphorus atom is bound to two alkyl or aryl groups such as in $[Ph_2P]^+$, which are commonly stabilised by the coordination of one or two Lewis bases[4] and ii) those in which

[a] Dr. J. M. Slattery, C. Fish, Prof. M. Green, T. N. Hooper, Dr. J. C. Jeffery, Dr. R. J. Kilby, Dr. C. A. Russell
School of Chemistry, University of Bristol
Cantock's Close, Bristol BS8 1TS (UK)
Fax: (+44) 117-929-0509
E-mail: michael804902@aol.com
Chris.Russell@bristol.ac.uk

[b] Dr. J. M. Lynam, Dr. C. E. Willans
Department of Chemistry, University of York
Heslington, York, YO10 5DD (UK)

[c] Prof. J. E. McGrady, Dr. D. A. Pantazis
WestCHEM, University of Glasgow, Joseph Black Building
Glasgow, G12 8QQ (UK)
Fax: (+44) 141-330-8261
E-mail: j.mcgrady@chem.gla.ac.uk

Supporting information for this article is available on the WWW under http://www.chemeurj.org/ or from the author.

the phosphorus atom is flanked by two amido moieties where the π-donating substituents serve to stabilise the nominally empty p orbital on the phosphorus center.[1a] These phosphenium cations are readily prepared by anion abstraction from a suitable precursor using a weakly-coordinating anion with (for the dialkyl- and diaryl-phosphenium salts) or without (for the amino-stabilised phosphenium cations) a Lewis base. The phosphenium cation can be used as a ligand to transition-metal centers[1b,5,6] either by carrying out the anion-abstraction reaction when the precursor is bound to the transition-metal center or by ligand-substitution reactions using "free" phosphenium ligand. Similar processes at phosphenium centers, whether they be the exchange of a π-bound ligand[7] or exchange of a coordinated terminal phosphine[8] have been the subject of recent interest, and clearly, it would help in the design of synthetic operations if we had a detailed understanding of the structure–activity relationships controlling the different reaction pathways.

In a series of recent papers we have used a combination of experimental and computational techniques to explore the properties of the tricyclic compound $ClP_3(CtBu)_2$ (**1**).[9] We showed that nucleophilic attack at **1** can occur via two distinct and competing pathways: an S_N2-type process involving direct substitution at the P-Cl phosphorus center and an addition–elimination (AE′) type process where the nucleophile attacks at one of the two phosphorus centers linked by a P–P bond.[9d] We have also demonstrated (Scheme 1) that **1** reacts with Lewis

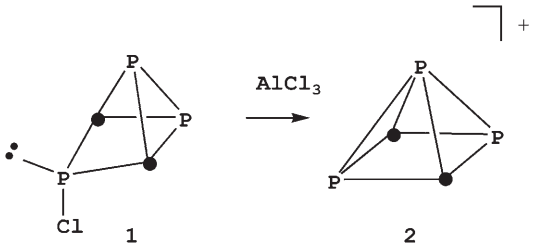

Scheme 1. ● = C*t*Bu.

acids, leading to the abstraction of Cl^- and the production of an ionic species containing the *nido*-[3,5-tBu_2-1,2,4-C_2P_3]$^+$ cation (**2**).[9a] This phosphorus–carbon cation is formally isoelectronic with $[C_5H_5]^+$, but its three-dimensional structure contrasts dramatically with the planar geometry of the all-carbon analogue,[9b] indicating that the phosphorus centers induce significant changes in the bonding. It was while attempting to access the monophosphorus analogue of these interesting five-atom cations that we isolated the novel phosphine–phosphenium adducts, $[R_2P{-}PR'_3]^+$ that are reported herein. In light of the considerable current interest in ligand exchange at these compounds, we use NMR spectroscopy to explore the mechanism of degenerate bimolecular substitution with excess PR'_3. We also use density functional theory to rationalise the structural properties of these phosphenium cations and establish the link between electronic structure and reactivity.

Results and Discussion

Synthesis: In seeking to gain access to cations of the type $[R_4C_4P]^+$, we attempted to abstract a chloride anion from the *P*-chlorophospholes Me_4C_4PCl (**3a**) and Et_4C_4PCl (**3b**) (Scheme 2), both of which are readily prepared by using an

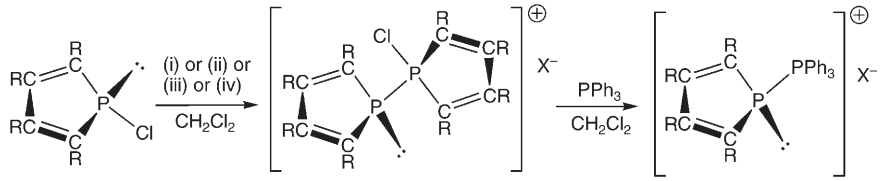

3 4 5

Scheme 2. i) ECl_3 (E = Al, Ga); ii) $Me_3SiOSO_2CF_3$, -Me_3SiCl; iii) $Ag[CB_{11}H_6Cl_6]$, -AgCl; iv) $Ag[Al\{OC(CF_3)_3\}_4]$, -AgCl.

adaptation of the Fagan–Nugent protocol.[10] However, halide abstraction using a variety of reagents (Group 13 trichlorides, $Me_3SiOSO_2CF_3$, or Ag^+ salts) gave products which feature a pair of mutual doublets with a large (ca. 300 Hz) P–P coupling constant in the $^{31}P\{^1H\}$ NMR spectra (Table 1), typical of P–P bonded species such as **4**.[11] The $^{31}P\{^1H\}$ NMR chemical shifts of the products were largely independent of the anion, suggesting minimal ion pairing. This solution-phase evidence is consistent with a mechanism in which i) the phosphenium cation, $[R_4C_4P]^+$, is formed and then trapped by a second *P*-chlorophosphole molecule or ii) P–Cl heterolysis occurs only after coordination of a second molecule of *P*-chlorophosphole, in which case the free phosphenium cation is never formed. Either hypothesis is also consistent with the fact that treatment of **3** with $Me_3SiOSO_2CF_3$ in the presence of one equivalent of PPh_3 afforded a quantitative yield of the phosphine–phosphenium

Table 1. $^{31}P\{^1H\}$ NMR data for derivatives of **4** and **5**.

Compound number	Cation	^{31}P NMR Chemical shifts [ppm]		$^1J_{PP}$ [Hz]
4a-$[AlCl_4]$	$[Me_4C_4P\{P(Cl)C_4Me_4\}]^+$	72.7	−21.4	372
4a-$[GaCl_4]$	$[Me_4C_4P\{P(Cl)C_4Me_4\}]^+$	72.7	−21.4	372
4b-$[AlCl_4]$	$[Et_4C_4P\{P(Cl)C_4Et_4\}]^+$	70.1	−27.9	390
4b-$[O_3SCF_3]$	$[Et_4C_4P\{P(Cl)C_4Et_4\}]^+$	98.8	−28.9	365
4b-$[CB_{11}H_6Cl_6]$	$[Et_4C_4P\{P(Cl)C_4Et_4\}]^+$	70.2	−27.7	390
4b-$[Al\{OC(CF_3)_3\}_4]$	$[Et_4C_4P\{P(Cl)C_4Et_4\}]^+$	70.2	−27.8	391
5a-$[AlCl_4]$	$[Me_4C_4P(PPh_3)]^+$	31.2	−36.8	300
5a-$[O_3SCF_3]$	$[Me_4C_4P(PPh_3)]^+$	31.5	−36.0	300
5b-$[O_3SCF_3]$	$[Et_4C_4P(PPh_3)]^+$	27.5	−47.4	311
5b-$[CB_{11}H_6Cl_6]$	$[Et_4C_4P(PPh_3)]^+$	27.8	−47.2	311
5b-$[Al\{OC(CF_3)_3\}_4]$	$[Et_4C_4P(PPh_3)]^+$	27.8	−47.1	311

adduct **5**, which is also formed on treatment of **4** with PPh_3 (Scheme 2, Table 1).

X-ray crystal structures: The identities of **5a**-$[O_3SCF_3]$ and **5b**-$[O_3SCF_3]$ were confirmed by single-crystal X-ray diffraction studies. The species are isostructural, showing separated $[R_4C_4P(PPh_3)]^+$ ion and triflate anion units (see Figure 1 for the structure of **5b**-$[O_3SCF_3]$; key bond lengths and angles for both **5a** and **5b** are given in Table 2). The structure of **5b**-$[O_3SCF_3]$ additionally contains a disordered molecule of CH_2Cl_2 in the lattice.

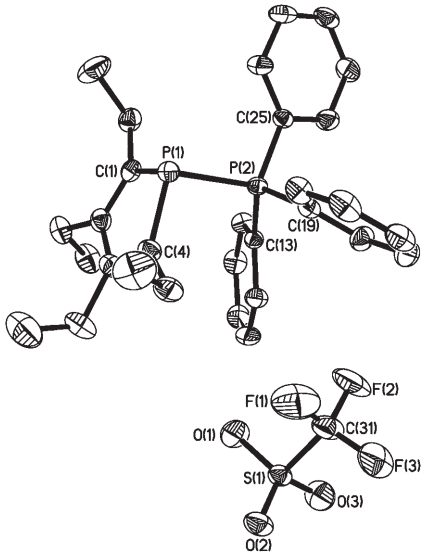

Figure 1. Molecular structure of $[Et_4C_4P(PPh_3)][OTf]$ (**5b**-$[O_3SCF_3]$). Thermal ellipsoids are displayed at the 40% probability level. Hydrogen atoms and the solvent of crystallisation (CH_2Cl_2) have been omitted for clarity.

The structures of **5a** and **5b** confirm the presence of the strong P–P bond (ca. 2.20 Å) anticipated from the ^{31}P-$\{^1H\}$ NMR spectra. The P–P bond lengths are very similar to those found in the $[PR_3–PPh_2]^+$ family characterised by Burford et al.,[11] but are almost 0.20 Å shorter than that in the $[ArNCH_2CH_2N(Ar)P(PMe_3)]^+$ ions reported by Baker and co-workers.[5] This dramatic change in structure hints at fundamental differences in the electronic distribution in these two classes of phosphenium cation, an issue that we explore in detail later in this paper. The C_4P rings in **5a** and **5b** are almost perfectly planar, and the crystal structures reveal clear evidence for an interaction between the ring and one of the phenyl groups: the angle between the two planes is about 31° with a torsion angle (defined by $C_4P_{centroid}$-P-P-$C_{ipso\text{-}phenyl}$) of only 2.1°, leading to inter-ring separations of only 3.2–3.5 Å. Furthermore, examination of the ^{13}C-$\{^1H\}$ NMR spectrum (CD_2Cl_2, 298 K) of **5b**-$[O_3SCF_3]$ reveals broadening of the signals in the aromatic region; although we have been unable to resolve this at lower temperatures and cannot unequivocally assign it as being due to the π–π interactions observed in the solid state, it is tempting to suggest that this is as a result of the maintenance on the NMR timescale of these interactions in solution which restricts the rotation of the PPh_3 group. We argue later that these π–π interactions have a significant influence on the kinetics of the phosphine–exchange reactions of the cations $[R_4C_4P\text{-}PR'_3]^+$.

Table 2. Selected bond lengths [Å] and angles [°] for **5a**-$[O_3SCF_3]$ and **5b**-$[O_3SCF_3]$.

	5a-$[O_3SCF_3]$	**5b**-$[O_3SCF_3]$
P(1)–P(2)	2.200(2)	2.1985(8)
C(1)–C(2)	1.344(9)	1.361(3)
C(2)–C(3)	1.45(1)	1.482(3)
C(3)–C(4)	1.357(9)	1.355(3)
P(1)–C(1)	1.798(6)	1.814(2)
P(1)–C(4)	1.812(6)	1.817(2)
C(1)-P(1)-C(4)	92.0(3)	92.5(1)
C(1)-P(1)-P(2)	95.5(2)	97.42(7)
C(4)-P(1)-C(2)	95.7(2)	97.49(8)

Kinetics of phosphine exchange: When PPh_3 (1 equiv) was added to a solution of **5b**-$[O_3SCF_3]$ in dichloromethane, the ^{31}P-$\{^1H\}$ NMR spectrum showed broadening of the resonances due to both coordinated and free PPh_3, which is consistent with exchange of the two PPh_3 environments on the NMR timescale. Importantly, we were also able to establish the rate of exchange between PPh_3 and **5b** by line-shape analysis using the gNMR suite of programmes[12] for each of the three ^{31}P-$\{^1H\}$ NMR resonances. As shown in Figure 2a the rate of exchange in CH_2Cl_2 at 293 K increases linearly with both [**5b**] and [PPh_3], implying net second-order kinetics (rate $= k_2[PPh_3][\mathbf{5b}]$), consistent with an associative (S_N2-type) pathway. An Eyring analysis (Figure 2b) over the temperature range 193–293 K afforded activation parameters of $\Delta S^{\neq} = (-106.3 \pm 6.7)\ J\,mol^{-1}\,K^{-1}$, $\Delta H^{\neq} = (14.9 \pm 1.6)\ kJ\,mol^{-1}$ and $\Delta G^{\neq}$ (298.15 K) $= (46.6 \pm 2.6)\ kJ\,mol^{-1}$. The negative entropy of activation is again diagnostic of an S_N2-type reaction, and the small value of $\Delta H^{\neq}$ suggests that the energy barrier for this reaction is entropically controlled. Unfortunately, all attempts to measure analogous data using other phosphenium–phosphine pairs proved unsuccessful as, to date, we have not been successful in isolating pure salts free from excess phosphine impurities. However, the characteristic broadness of the ^{31}P-$\{^1H\}$ NMR signals associated with free and coordinated phosphine is observed in all samples, suggesting that exchange is rapid.

The evidence for S_N2-type kinetics detailed in the preceding paragraph stands in stark contrast to the dominant S_N1-type pathway reported by Baker and co-workers for the analogous exchange reaction in the $[ArNCH_2CH_2N(Ar)P(PMe_3)]^+$ ion.[5a] The trend towards an associative, rather than dissociative, pathway in **5a** and **5b** is consistent with the shorter P–P bond lengths in these compounds compared to the Baker systems, and suggests a fundamentally different distribution of electron density at the electron-deficient phosphorus center. The electronic structure of phosphenium cations and their adducts with a variety of Lewis bases has

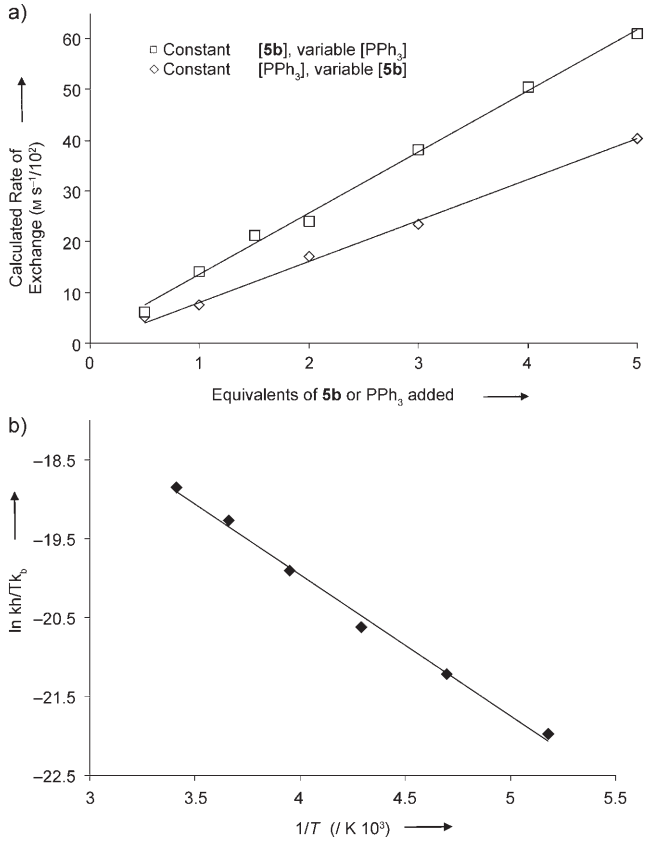

Figure 2. a) Effect of **5b** and [PPh_3] on the rate of exchange. b) Eyring plot for the exchange of free and coordinated PPh_3 (rate data obtained from simulation of the coordinated PPh_3 resonance).

been discussed in a number of recent papers.[7b,13,14] The majority of this work has focussed on simple models for the Baker system such as $[(H_2N)_2P]^+$, in which the cationic phosphorus center is strongly stabilised by the π-orbitals on the amide substituent. Macdonald and co-workers have also compared the Lewis acidity of this species with the diphenyl analogue, $[Ph_2P]^+$, and concluded that a phenyl group is unable to delocalise the positive charge effectively, leading to much stronger P–P bonds in the phosphine adducts.[14] To understand more fully the apparently different reaction paths followed by **5b** and the Baker systems, we have used density functional theory to compare the electronic structure of $[Et_4C_4P(PPh_3)]^+$, and the amide-substituted species $[ArNCH_2CH_2N(Ar)P(PMe_3)]^+$.

Electronic structure: The optimised geometry of the phosphenium cation, $[Et_4C_4P]^+$, is shown in Figure 3, along with that of its phosphine adduct, $[Et_4C_4P(PPh_3)]^+$ (**5b**). The optimised structures of the diphenyl phosphenium cation, $[PPh_2]^+$ and the amide-substituted species, $[ArNCH_2CH_2N(Ar)P]^+$ are also shown in Figure 3 for comparison, along with their respective adducts, $[PPh_2(PPh_3)]^+$ and $[ArNCH_2CH_2N(Ar)P(PMe_3)]^+$. The bond lengths within the five-membered rings in the bare phosphenium cations, $[Et_4C_4P]^+$ and $[ArNCH_2CH_2N(Ar)P]^+$, immediately confirm a distinct difference in electronic structure at the phosphorus centre: in the former, the C–P bond lengths (1.78 Å) are typical of single bonds, while the alternation of the C–C bond lengths (1.36 Å, 1.54 Å) is typical of a localised 1,3-butadienyl fragment. The structural features therefore suggest that the LUMO is strongly localised on the phosphorus centre, with minimal delocalisation into the butadiene π-system, a picture that is confirmed by the Wiberg indices of 0.94 and 1.78 for the P–C and C=C bonds, respectively. In contrast, the P–N bond lengths in $[ArNCH_2CH_2N(Ar)P]^+$ (1.62 Å) are rather short, and the Wiberg index of 1.09 confirms the presence of significant π character due to donation of electrons from the amide group into the vacant p orbital on the phosphorus centre.

We noted in the introductory paragraph that the phosphenium cations are isolobal to the carbenes, and the structural features highlighted in the previous paragraph suggest that while $[ArNCH_2CH_2N(Ar)P]^+$ resembles a mesomerically stabilised "Fischer" carbene, the absence of π-donor groups in $[Et_4C_4P]^+$ suggests a closer link to a "Schrock"-type carbene. The Fischer/Schrock distinction in carbene chemistry is often discussed in terms of the separation between singlet and triplet states of the free ligand[15] which, in turn, is determined by the stability of the p orbital that is vacant in the

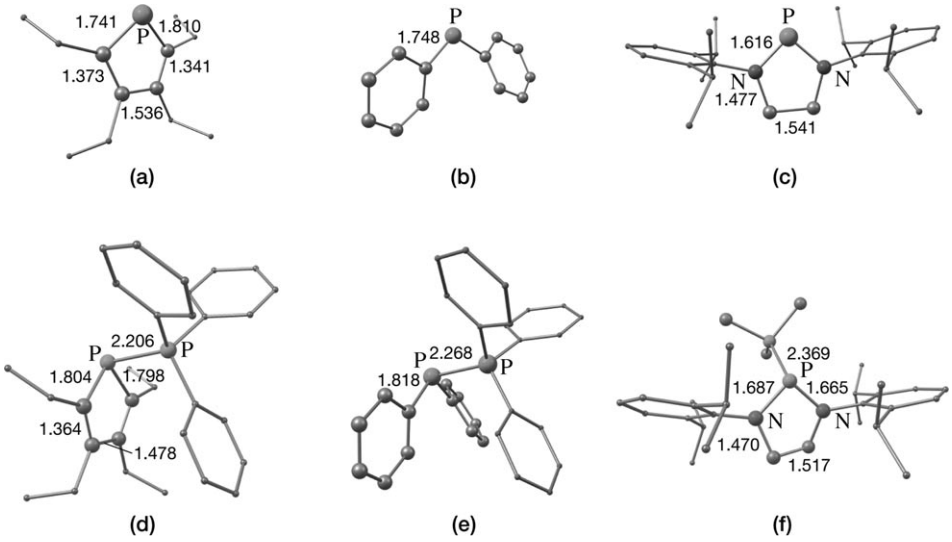

Figure 3. Optimized structures of the three phosphenium cations $[Et_4C_4P]^+$ (a), $[PPh_2]^+$ (b) and $[ArNCH_2CH_2N(Ar)P)]^+$ (c) and their phosphine adducts, $[Et_4C_4P(PPh_3)]^+$ (d), $[PPh_2(PPh_3)]^+$ (e) and $[ArNCH_2CH_2N(Ar)P(PMe_3)]^+$ (f). In each structure, the QM partition is shown as ball-and-stick, MM partition as sticks.

singlet. Thus, carbenes with relatively low-lying triplet states tend to exhibit Schrock-type character when complexed to metal centres, while those with high-lying triplet states tend to form Fischer-type complexes. Both $[H_4C_4P]^+$ and $[HNCH_2CH_2N(H)P]^+$ adopt singlet ground states, but the lowest triplet states lie 64 kJ mol^{-1} and 253 kJ mol^{-1} higher, respectively, providing a clear indication that the bonding in adducts of $[R_4C_4P]^+$ will bear closer resemblance to the Schrock limit in carbene chemistry. This simple analogy proves very useful in rationalising the structural and reaction chemistry of the adducts.

For the three phosphine–phosphenium adducts shown in Figure 3, agreement between optimised and crystallographic bond lengths is in all cases acceptable. In particular, the calculations reproduce the experimental trend in P–P bond lengths: $[Et_4C_4P(PPh_3)]^+$ (2.21 Å) < $[Ph_2P(PPh_3)]^+$ (2.27 Å) < $[ArNCH_2CH_2N(Ar)P(PMe_3)]^+$ (2.37 Å). Importantly, the calculations also reproduce the stacking of the C_4P ring with one of the phenyl groups noted in the crystal structures of **5a** and **5b**. As might be anticipated based on the minimal delocalisation of the positive charge onto the butadiene component of the five-membered ring, the formation of the P–P bond in $[Et_4C_4P(PPh_3)]^+$ has only minimal impact on the C–P bonds within the R_4C_4P ring, (1.78 Å vs. 1.80 Å, av). In contrast, the formation of the P–P bond in $[ArNCH_2CH_2N(Ar)P(PMe_3)]^+$ causes a 0.07 Å elongation of the P–N bonds, reflecting the competition between the phosphine lone pair and the amide π-electrons for the formally vacant p orbital on the phosphorus centre. The P–P bond lengths and the associated structural changes within the phosphenium units again highlight the analogy with Fischer/Schrock carbenes: the short P–P bonds in $[Et_4C_4P(PPh_3)]^+$ mimic the strong M=C π-bonding in Schrock carbenes, while the weaker N=P bonding in $[ArNCH_2CH_2N(Ar)P(PMe_3)]^+$ is reminiscent of the changes in heteroatom–carbon bonding that occur upon coordination of a typical Fischer carbene.

In the context of phosphine exchange, the P–P bond dissociation energy can be related to the barrier for an S_N1-type process. The loss of PPh_3 from $[Et_4C_4P(PPh_3)]^+$ is far more endoergic ($\Delta G = +286$ kJ mol^{-1}) than the loss of PMe_3 from $[ArNCH_2CH_2N(Ar)P(PMe_3)]^+$ ($\Delta G = +50$ kJ mol^{-1}) confirming that the S_N1-type pathway is much more facile in the latter. The comparison of the two species is fully consistent with the work of Macdonald and co-workers who showed that adducts of $[Ph_2P]^+$ with PMe_3 are more strongly bound than those of $[(Me_2N)_2P]^+$.[14] However, the difference between $[ArNCH_2CH_2N(Ar)P(PMe_3)]^+$ and $[Et_4C_4P(PPh_3)]^+$ is much more pronounced than that between $[Ph_2P]^+$ and $[(Me_2N)_2P]^+$ ($\Delta(\Delta G) = 236$ kJ mol^{-1} vs. 130 kJ mol^{-1}), suggesting that the presence of π-donating amide groups is not the sole factor that influences the dissociation energies. We have previously noted the stacking of the π systems of the C_4P ring and one phenyl group in $[Et_4C_4P(PPh_3)]^+$, and anticipated that it may have a stabilising effect on the adduct. There are no similarly stabilising secondary interactions in $[ArNCH_2CH_2N(Ar)P(PMe_3)]^+$, and indeed it is clear from the optimised structure that the phosphine ligand occupies a very sterically crowded site. To separate the influence of these secondary steric interactions from the intrinsic strength of the P–P bonds, we have repeated these calculations using the simplified model systems $[H_4C_4P(PH_3)]^+$ and $[HNCH_2CH_2N(H)P(PMe_3)]^+$. The optimised P–P bond length in $[H_4C_4P(PH_3)]^+$ (2.17 Å) is marginally shorter than in **5a** and **5b**, but despite this the free energy for phosphine dissociation is significantly *reduced* ($\Delta G = +222$ kJ mol^{-1} vs. $+286$ kJ mol^{-1} for the full system). It should be emphasised that, as a consequence of our chosen QM/MM partition for $[Et_4C_4P(PPh_3)]^+$, the inductive effects of the phenyl groups are not accounted for in our model. In electronic terms, the phosphine ligand is therefore identical to PH_3 and the difference of 64 kJ mol^{-1} in the ligand dissociation energy can be attributed directly to π–π interactions between the phenyl group and $[C_4P]^+$ ring. The magnitude of the π–π interactions can also be estimated by rotating the PPh_3 unit by 180° about the P–P bond, thereby eliminating the stacking interaction. This partially optimised structure lies 64 kJ mol^{-1} above the equilibrium geometry, confirming our estimate of the magnitude of the π–π interactions. In the model system $[HNCH_2CH_2N(H)P(PMe_3)]^+$, the P–P bond length is also shorter than in the fully substituted compound (2.27 Å vs. 2.37 Å), but the phosphine dissociation free energy *increases* from 50 kJ mol^{-1} to 85 kJ mol^{-1}, indicating that the secondary steric interactions are destabilising in this case.

Whilst S_N1-type mechanisms for this class of complex have been extensively discussed, S_N2-type kinetics, and specifically the $[R_3P\text{-}PR'_2\text{-}PR_3]^+$ adducts that relate to the transition state, have received little attention. A theoretical study of the reaction $[{}^*PH_3{-}PH_2]^+ + PH_3 \rightarrow [PH_3{-}PH_2]^+ + {}^*PH_3$ concluded that an associative pathway is possible, but attempts to confirm this through kinetic measurements have so far been frustrated by rapid rates of reaction and long ^{31}P relaxation times.[8] To the best of our knowledge, there have been no attempts to make a direct comparison of associative (S_N2-type) and dissociative (S_N1-type) pathways in phosphine-phosphenium cations.

Addition of a second phosphine ligand to $[Et_4C_4P(PPh_3)]^+$ gives a weak encounter complex, $[(PPh_3)\cdots Et_4C_4P(PPh_3)]^+$, with a very long P–P distance of 2.94 Å. Further along the reaction coordinate (Figure 4), we have located a classic S_N2-type transition state with two equivalent P–P bonds (2.59 Å), which lies only 16 kJ mol^{-1} above the separated reactants. The transition state in the corresponding model system $[(PH_3)\cdots H_4C_4P(PH_3)]^+$ lies 18 kJ mol^{-1} above the separated reactants, suggesting that, in marked contrast to the S_N1-type process, π–π interactions do *not* contribute significantly to the barrier in the S_N2-type pathway.

The difference between the two mechanisms can be traced to the nature of the structural changes along the reaction coordinate: In the S_N1-type process, the π–π interaction is lost completely in the rate-limiting step, while in the S_N2-type reaction pathway the progressive loss of π–π stabilization with the departing phosphine is compensated by the in-

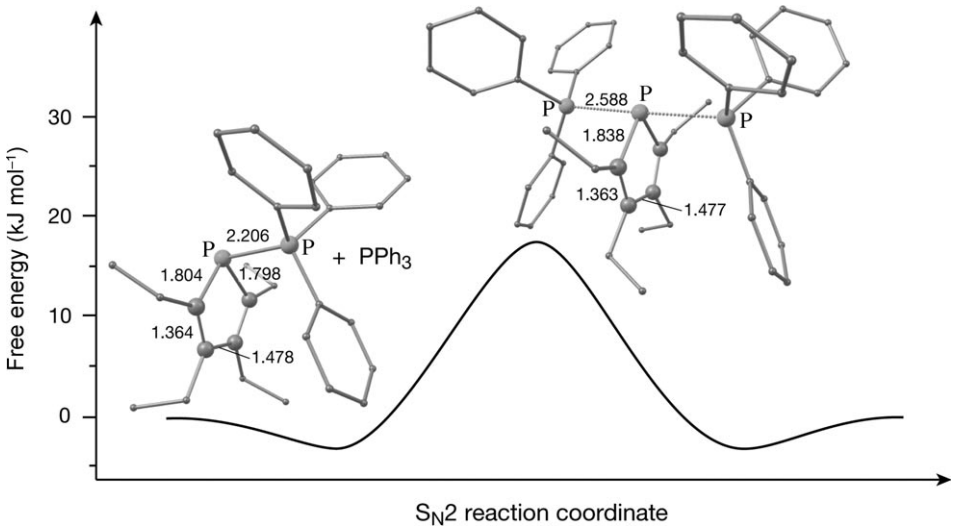

Figure 4. S_N2-type pathway for phosphine exchange in $[Et_4C_4P(PPh_3)]^+$.

creasing interaction with the incoming phosphine. As a result, the energetic contribution of π–π stacking remains approximately constant across the entire S_N2-type reaction coordinate, and so the removal of the phenyl groups does not influence the barrier height to any great extent.

Having established that S_N2-type kinetics are more favorable in the $[Et_4C_4P(PPh_3)]^+ + PPh_3$ system, we must finally consider why the corresponding pathway is apparently not observed for the reaction of PMe_3 with $[ArNCH_2CH_2N(Ar)P(PMe_3)]^+$. In fact, we have been unable to locate either a precursor complex or an S_N2-type transition state for this system, probably due to the extreme steric crowding at the phosphenium cation. The isopropyl substituents at the *ortho* positions of the aryl rings are particularly significant, as they effectively block the path of an incoming nucleophile. Moreover, the departing PMe_3 group prevents rotation about the N–C bonds which would move these bulky groups into a less crowded position. When the aryl groups are removed, the potential energy surface for the S_N2-type pathway for $[(PMe_3)\cdots HNCH_2CH_2N(H)P(PMe_3)]^+$ closely resembles that shown in Figure 4, with a transition state 16 kJ mol^{-1} higher than the separated reactants.[16] The barrier is therefore very similar to that in $[(PPh_3)\cdots Et_4C_4P(PPh_3)]^+$, a dramatic contrast to the corresponding S_N1-type pathway where, as we have shown above, the π-donor character of the amide groups plays a key role. In the S_N2-type pathway, however, the phosphorus centre remains electronically saturated across the entire reaction coordinate, and so π-donation is less important. On this basis, we conclude that the absence of a viable S_N2-type pathway for the amide-substituted phosphenium cation is entirely due to the steric bulk of the aryl groups.

Conclusions

In summary, we have shown that abstraction of a Cl^- ion from the *P*-chlorophospholes, R_4C_4PCl (R = Me, Et) produces species containing the $[R_4C_4P–P(Cl)C_4R_4]^+$ ion, which in the presence of PPh_3 affords the phosphine–phosphenium cations $[R_4C_4P(PPh_3)]^+$ (R = Me, Et). Addition of excess PPh_3 leads to exchange of free- and coordinated-phosphine ligands, and importantly, we have shown experimentally that this process occurs with second order kinetics, in marked contrast to the dominant dissociative (S_N1-type) pathway reported[5a] for the analogous exchange reactions of the $[ArNCH_2CH_2N(Ar)P(PMe_3)]^+$ ion. DFT calculations have allowed us to probe the factors controlling these two different reaction pathways, and show that whilst phosphine exchange in $[Et_4C_4P(PPh_3)]^+$ and $[ArNCH_2CH_2N(Ar)P(PMe_3)]^+$ are superficially similar, they differ significantly in both their electronic and steric requirements. The highly electrophilic phosphorus center in $[Et_4C_4P]^+$, combined with strong π–π interactions between the ring and the incoming and outgoing phenyl groups of PPh_3, favours the S_N2-type over the S_N1-type pathway in $[Et_4C_4P(PPh_3)]^+$. In contrast, more effective π-donation from the amide groups reduces the intrinsic electrophilicity in $[ArNCH_2CH_2N(Ar)P]^+$, which when combined with the steric bulk of the aryl groups, shifts the mechanism in favour of a dissociative S_N1-type pathway.

Experimental Section

General: All reactions were conducted by using standard inert atmosphere (Schlenk line and glove box) techniques. Solvents (toluene, dichloromethane, *n*-hexane) were purified using the system described by Grubbs et al.[17] The *P*-chlorophospholes, R_4C_4PCl (R = Me, **3a**; Et, **3b**) were made by literature procedures;[10] **3a** was produced and allowed to react in situ, whereas **3b** was stored and used as a 1 M solution in *n*-hexane. $AlCl_3$ was purchased from Aldrich and sublimed twice immediately prior to use. $GaCl_3$ and $Me_3SiOSO_2CF_3$ were purchased from commercial sources and used as supplied. $Ag[Al\{OC(CF_3)_3\}_4]$ was prepared by the literature route[18] and $Ag[CB_{11}H_6Cl_6]$ was supplied by Dr. A. S. Weller (University of Bath) and used as received.

Synthesis of 4 and 5: In a typical procedure, R_4C_4PCl (2 mmol) was dissolved in CH_2Cl_2 (30 mL), cooled to 0 °C and allowed to react with an equimolar amount of the relevant halide abstraction reagent ($AlCl_3$, $GaCl_3$, $Me_3SiOSO_2CF_3$ or $Ag[Al\{OC(CF_3)_3\}_4]$). Note that when reactions were carried out using $Ag[CB_{11}H_6Cl_6]$ as the halide abstraction reagent, the scale was reduced to 0.05 mmol in CH_2Cl_2 (3 mL). Following halide abstraction, all reactions gave yellow solutions whose ^{31}P NMR spectra were characteristic of the phosphine–phosphenium cations, $[R_4C_4P–$

$P(Cl)C_4R_4]^+$ (**4**). These solutions were then allowed to react with an equimolar amount of PPh_3 to give colourless to very pale yellow solutions containing the cations $[R_4C_4P{-}PPh_3]^+$ (**5**).

Data for 5a-[O_3SCF_3]: X-ray quality crystals were produced by removing the volatiles in vacuo to give a pale cream solid, which was suspended in Et_2O (10 mL) and re-dissolved with CH_2Cl_2 (4 mL). Storage of this solution at −15 °C overnight gave light yellow blocks of **5a**-[O_3SCF_3] (0.762 g; 63 %). ^{1}H NMR (+25 °C, 300 MHz, CD_2Cl_2): δ = 7.74–7.52 {collection of overlapping m, 15H, -P(C_6H_5)$_3$}, 1.67 (d, $^3J_{H,P}$ = 9 Hz, 6H; -PC(α)CH_3), 1.48 ppm (s, 6H; -C(β)CH_3); ^{31}P-{^{1}H} NMR (+25 °C, 121.4 MHz, CD_2Cl_2): δ = 31.5 (d, $^1J_{P,P}$ = 300 Hz; -PPh_3), −36.0 ppm (d, $^1J_{P,P}$ = 300 Hz; -PC_4Me_4); ^{13}C NMR (+25 °C, 75.5 MHz, CD_2Cl_2): δ = 156.5 (d, $^2J_{P,C}$ = 7 Hz; C(ß)), 133.6 (d, $^2J_{C,P}$ = 16 Hz; C(α)), 121.1 (q, $^1J_{F,C}$ = 321 Hz; SO_3CF_3), 14.5 (d, $^3J_{C,P}$ = 2 Hz; -C(ß)CH_3), 14.2 ppm (d, $^2J_{P,C}$ = 20 Hz; -C(α)CH_3); elemental analysis calcd (%) for [$Me_4C_4P(PPh_3)$]-[O_3SCF_3]: C 58.91, H 4.91; found: C 58.49, H 4.58.

Data for 5b-[O_3SCF_3]: X-ray quality crystals were produced by removing the volatiles in vacuo to give a pale cream solid, which was suspended in Et_2O (10 mL) and re-dissolved with CH_2Cl_2 (2 mL). Storage of this solution at −15 °C overnight gave 0.762 g (63 %) of colorless blocks of **5b**-[O_3SCF_3]$^-$. M.p.: 138–141 °C; ^{1}H NMR (+25 °C, 300 MHz, CD_2Cl_2): δ = 7.76–7.55 {collection of overlapping m, 15H; -P(C_6H_5)$_3$}, 2.50–1.50 (collection of overlapping m, 8H, -CH_2CH_3), 1.03 (t, $^3J_{H,H}$ = 7.5 Hz, 6H; -CH_2CH_3), 0.65 (t, $^3J_{H,H}$ = 7.6 Hz, 6H; -CH_2CH_3) ppm; ^{31}P-{^{1}H} NMR (+25 °C, 121.4 MHz, CD_2Cl_2): δ = 27.5 (d, $^1J_{P,P}$ = 310 Hz; -PPh_3), −47.3 (d, $^1J_{P,P}$ = 310 Hz; -PC_4Et_4) ppm; ^{13}C NMR (+25 °C, 75.5 MHz, CD_2Cl_2): δ = 162.4 (d, $^2J_{P,C}$ = 8 Hz; -PCEt*C*Et), 137.0 (br, s; PPh_3-C_1), 136.2 (d, $^4J_{P,C}$ = 11 Hz; PPh_3-C_4), 135.0 (br, s; PPh_3-C_2), 136.2 (d, $^3J_{P,C}$ = 12 Hz; PPh_3-C_3), 123.0 (q, $^1J_{C,F}$ = 321 Hz; O_3SCF_3), 120.5 (br. d, $^1J_{P,C}$ = 74 Hz; -P*C*EtCEt), 23.8 (d, $^2J_{P,C}$ = 18 Hz; -PC{CH_2CH_3}CEt), 23.5 (d, $^3J_{P,C}$ = 2 Hz; -PCEtC-{CH_2CH_3}), 19.0 (d, $^3J_{P,C}$ = 6 Hz; -PC{CH_2CH_3}CEt), 16.0 (s; PCEtC-{CH_2CH_3}) ppm; elemental analysis calcd (%) for [$Et_4C_4P(PPh_3)$]-[O_3SCF_3]: C 61.38, H 5.82; found: C 61.25, H 5.83.

Kinetic data: The rate of phosphine exchange was obtained by line shape analysis using the gNMR suite of programmes for each of the three resonances in the ^{31}P-{^{1}H} NMR spectrum.[12] Spectra were recorded of a constant concentration (1.25×10^{-1} M) of PPh_3 in dichloromethane at 293 K, and the concentration of **5b** was increased from 6.26×10^{-2} M to 6.26×10^{-1} M. The dependence of the rate of exchange on the concentration of PPh_3 was performed in a similar manner with a constant concentration of **5b**.

Activation parameters were determined by recording a series of spectra of an equimolar solution of **5b** and PPh_3 over the temperature range 193–273 K. Excellent fits to the experimental data for the resonance due to the coordinated PPh_3 group were obtained. These data were employed to generate Eyring plots which afforded activation parameters of $\Delta S^{\neq} = (-106.3\pm6.7)$ J mol^{-1} K^{-1} and $\Delta H^{\neq} = (14.9\pm1.6)$ kJ mol^{-1} with R^2 = 0.99.

Single-crystal X-ray diffraction data: X-ray measurements were made using a Bruker SMART CCD area-detector diffractometer with $Mo_{K\alpha}$ radiation (λ = 0.71073 Å). Structures were solved by Direct Methods and refined by full matrix least squares refinement on F^2. Absorption corrections were applied based on multiple and symmetry-equivalent measurements. All non-hydrogen atoms were assigned anisotropic displacement parameters and refined without positional constraints. All hydrogen atoms were constrained to ideal geometries and refined with fixed isotropic displacement parameters. CCDC-280172 and CCDC-629273 contain the supplementary crystallographic data for this paper. These data can be obtained free of charge from the Cambridge Crystallographic Data Centre via www.ccdc.cam.ac.uk/data_request/cif.

Data for 5a-[O_3SCF_3]: $C_{27}H_{27}F_3O_3P_2S$. M = 550.49, monoclinic, space group $P2/c$, Z = 4, a = 18.505(1), b = 9.4777(6), c = 15.213(1) Å, β = 94.780(1)°, V = 2658.8(3) Å^3, crystal size 0.35x0.31x0.25 mm, ρ_{calcd} = 1.375 g cm^{-3}, $\mu(Mo_{K\alpha})$ = 0.291 mm^{-1}, T = 100(2) K. The total dataset was a sphere. Of a total of 27694 reflections collected, 6118 were independent (R_{int} = 0.0882). R_1 = 0.0940 [for all 3239 reflections with $I > 2\sigma(I)$] and wR_2 = 0.3057 for all data.

Data for 5b-[O_3SCF_3]: $C_{32}H_{37}Cl_2F_3O_3P_2S$, M = 691.52, triclinic, space group $P\bar{1}$, Z = 2, a = 9.2702(5), b = 11.1171(6), c = 16.8889(9) Å, α = 2.3670(10), β = 85.1890(10), γ = 89.9080(10)°, V = 1718.95(16) Å^3, crystal size 0.40 × 0.25 × 0.20 mm, ρ_{calcd} = 1.336 g cm^{-3}, $\mu(Mo_{K\alpha})$ = 0.390 mm^{-1}, T = 173(2) K. The total data set was a sphere. Of a total of 18398 reflections collected, 7800 were independent (R_{int} = 0.0264). Final R_1 = 0.0492 [for 6139 reflections with $I > 2\sigma(I)$] and wR_2 = 0.1598 (all data).

Computational details: Hybrid quantum mechanics/molecular mechanics (QM/MM) calculations were performed by using the ONIOM implementation in Gaussian 03.[19] For the QM part the PBE1PBE hybrid density functional[20] was used in conjunction with 6–311G(d) basis sets for C, N, and H atoms[21] and the McLean-Chandler triple-ζ basis set for phosphorus,[22] augmented with two sets of *d* and one set of *f* polarization functions. The UFF force field[23] was employed for the MM part. For the $[Et_4C_4P]^+$-PPh_3 system, the QM partition was defined as $[H_4C_4P]^+$ and PH_3, while for $[Ph_2P]^+$-PPh_3, it was $[Ph_2P]^+$ and PH_3. This QM/MM partition means that the PPh_3 ligand is, in terms of its electronic properties, effectively the same as PH_3. The electronic properties of phosphine ligands, PR_3, have been discussed in terms of the minimum value of the molecular electrostatic potential (V_{min}), which correlates well with the pK_a value of the corresponding conjugate acids, $[PR_3H]^+$.[24] Values of V_{min} for PH_3 and PPh_3 are rather similar (−118.1 kJ mol^{-1} and −145.8 kJ mol^{-1}, respectively), suggesting that our chosen QM/MM partition provides a reasonable representation of the electronic properties of the ligand. V_{min} for PMe_3 (−180.0 kJ mol^{-1}) is, in contrast, much more negative, indicating that a similar QM/MM partition across the P–C bonds will substantially underestimate the electron-donating power of the phosphorus center. As a result, we have chosen to treat the Me groups in the amido phosphine quantum mechanically, giving a QM partition of $[HNCH_2CH_2N(H)P]^+$ and PMe_3. Reaction pathways for the simplified models were computed at the PBE1PBE level with the same basis sets. The optimized stationary points were characterized as minima or transition states by analytic vibrational frequency calculations at the same level of theory and the final energies reported include zero-point and thermal free energy corrections at 298.15 K and 1 atm.

Acknowledgements

We thank the Royal Society (University Research Fellowship for C.A.R.), the University of Bristol (M.G., C.A.R., C.F., J. M.S.) and the EPSRC (R.J.K., D.A.P., C.E.W.) for financial support. In addition we thank Dr. A. S. Weller (University of Bath) for kindly supplying us with $Ag[CB_{11}H_6Cl_6]$.

[1] a) A. H. Cowley, R. A. Kemp, *Chem. Rev.* **1985**, *85*, 367–382; b) D. Gudat, *Coord. Chem. Rev.* **1997**, *163*, 71–106; c) N. Burford, P. J. Ragogna, *Dalton Trans.* **2002**, 4307–4315.

[2] a) A. J. Arduengo, *Acc. Chem. Res.* **1999**, *32*, 913–921; b) D. Bourissou, O. Guerret, F. P. Gabbai, G. Bertrand, *Chem. Rev.* **2000**, *100*, 39–92.

[3] M. Driess, H. Grützmacher, *Angew. Chem.* **1996**, *108*, 900–929; *Angew. Chem. Int. Ed. Engl.* **1996**, *35*, 828–856.

[4] a) C. W. Schultz, R. W. Parry, *Inorg. Chem.* **1976**, *15*, 3046–3050; b) N. Burford, T. S. Cameron, P. J. Ragogna, E. Ocando-Mavarez, M. Gee, R. McDonald, R. E. Wasylishen, *J. Am. Chem. Soc.* **2001**, *123*, 7947–7948.

[5] a) See M. B. Abrams, B. L. Scott, R. T. Baker, *Organometallics* **2000**, *19*, 4944–4956, and references 30–66 therein. b) N. J. Hardman, M. B. Abrams, M. A. Pribisko, T. M. Gilbert, R. L. Martin, G. B. Kubas, R. T. Baker, *Angew. Chem.* **2004**, *116*, 1989–1992; *Angew. Chem. Int. Ed.* **2004**, *43*, 1955–1958.

[6] See H. Nakazawa, *J. Organomet. Chem.* **2000**, *611*, 349–363, and references therein.

[7] a) D. C. R. Hockless, M. A. McDonald, M. Pabel, S. B. Wild, *J. Organomet. Chem.* **1997**, *538*, 189–196; b) T. I. Sølling, M. A. McDonald, S. B. Wild, L. Radom, *J. Am. Chem. Soc.* **1998**, *120*, 7063–7068.

[8] T. I. Sølling, S. B. Wild, L. Radom, *Inorg. Chem.* **1999**, *38*, 6049–6054.
[9] a) J. M. Lynam, M. C. Copsey, M. Green, J. C. Jeffery, J. E. McGrady, C. A. Russell, J. M. Slattery, A. C. Swain, *Angew. Chem.* **2003**, *115*, 2884–2888; *Angew. Chem. Int. Ed.* **2003**, *42*, 2778–2782; b) D. A. Pantazis, J. E. McGrady, J. M. Lynam, C. A. Russell, M. Green, *Dalton Trans.* **2004**, 2080–2086; c) C. Fish, M. Green, J. C. Jeffery, R. J. Kilby, J. M. Lynam, C. A. Russell, C. E. Willans, *Organometallics* **2005**, *24*, 5789–5791; d) C. Fish, M. Green, R. J. Kilby, J. M. Lynam, J. E. McGrady, D. A. Pantazis, C. A. Russell, A. C. Whitwood, C. E. Willans, *Angew. Chem.* **2006**, *118*, 3710–3713; *Angew. Chem. Int. Ed.* **2006**, *45*, 3628–3631.
[10] P. J. Fagan, W. A. Nugent, *J. Am. Chem. Soc.* **1988**, *110*, 2310–2312.
[11] N. Burford, P. J. Ragogna, R. McDonald, M. J. Ferguson, *J. Am. Chem. Soc.* **2003**, *125*, 14404–14410.
[12] gNMR, version 5.0.5.0, Ivory Software, **2005**.
[13] a) R. J. Boyd, N. Burford, C. L. B. Macdonald, *Organometallics* **1998**, *17*, 4014–4029; b) D. Gudat, *Eur. J. Inorg. Chem.* **1998**, 1087–1094; c) D. Gudat, A. Haghverdi, H. Hupfer, M. Nieger, *Chem. Eur. J.* **2000**, *6*, 3414–3425.
[14] B. D. Ellis, P. J. Ragogna, C. L. B. Macdonald, *Inorg. Chem.* **2004**, *43*, 7857–7867.
[15] M. Lein, A. Szabo, A. Kovacs, G. Frenking, *Faraday Discuss.* **2003**, *124*, 365–378.
[16] Due to SCF convergence problems, it proved impossible to optimise the transition state using the [2d,1f] polarized basis set for phosphorus. The estimate for the barrier is instead obtained using the analogous basis set with a single set of d polarization functions. A parallel set of calculations on the $[(PH_3)\cdots C_4H_4P(PH_3)]^+$ system, where no such convergence problems were encountered, suggests that the change in basis set changes the barrier by less than 10 kJ mol^{-1}.
[17] A. B. Pangborn, M. A. Giardello, R. H. Grubbs, R. K. Rosen, F. J. Timmers, *Organometallics* **1996**, *15*, 1518–1520.
[18] I. Krossing, *Chem. Eur. J.* **2001**, *7*, 490–502.
[19] Gaussian 03, Revision D.02, M. J. Frisch, G. W. Trucks, H. B. Schlegel, G. E. Scuseria, M. A. Robb, J. R. Cheeseman, J. A. Montgomery, Jr., T. Vreven, K. N. Kudin, J. C. Burant, J. M. Millam, S. S. Iyengar, J. Tomasi, V. Barone, B. Mennucci, M. Cossi, G. Scalmani, N. Rega, G. A. Petersson, H. Nakatsuji, M. Hada, M. Ehara, K. Toyota, R. Fukuda, J. Hasegawa, M. Ishida, T. Nakajima, Y. Honda, O. Kitao, H. Nakai, M. Klene, X. Li, J. E. Knox, H. P. Hratchian, J. B. Cross, V. Bakken, C. Adamo, J. Jaramillo, R. Gomperts, R. E. Stratmann, O. Yazyev, A. J. Austin, R. Cammi, C. Pomelli, J. W. Ochterski, P. Y. Ayala, K. Morokuma, G. A. Voth, P. Salvador, J. J. Dannenberg, V. G. Zakrzewski, S. Dapprich, A. D. Daniels, M. C. Strain, O. Farkas, D. K. Malick, A. D. Rabuck, K. Raghavachari, J. B. Foresman, J. V. Ortiz, Q. Cui, A. G. Baboul, S. Clifford, J. Cioslowski, B. B. Stefanov, G. Liu, A. Liashenko, P. Piskorz, I. Komaromi, R. L. Martin, D. J. Fox, T. Keith, M. A. Al-Laham, C. Y. Peng, A. Nanayakkara, M. Challacombe, P. M. W. Gill, B. Johnson, W. Chen, M. W. Wong, C. Gonzalez, J. A. Pople, Gaussian, Inc., Wallingford CT, **2004**.
[20] a) J. P. Perdew, K. Burke, M. Ernzerhof, *Phys. Rev. Lett.* **1996**, *77*, 3865–3868; b) J. P. Perdew, K. Burke, M. Ernzerhof, *Phys. Rev. Lett.* **1997**, *78*, 1396; c) C. Adamo, V. Barone, *J. Chem. Phys.* **1999**, *110*, 6158–6170.
[21] R. Krishnan, J. S. Binkley, R. Seeger, J. A. Pople, *J. Chem. Phys.* **1980**, *72*, 650–654.
[22] A. D. McLean, G. S. Chandler, *J. Chem. Phys.* **1980**, *72*, 5639–5648.
[23] A. K. Rappé, C. J. Casewit, K. S. Colwell, W. A. Goddard III, W. M. Skiff, *J. Am. Chem. Soc.* **1992**, *114*, 10024–10035.
[24] a) C. H. Suresh, N. Koga, *Inorg. Chem.* **2002**, *41*, 1573–1578; b) O. Kûhl, *Coord. Chem. Rev.* **2005**, *249*, 693–704.

Received: December 5, 2006
Published online: May 31, 2007

